Engineering Notes

ENGINEERING NOTES are short manuscripts describing new developments or important results of a preliminary nature. These Notes cannot exceed 6 manuscript pages and 3 figures; a page of text may be substituted for a figure and vice versa. After informal review by the editors, they may be published within a few months of the date of receipt. Style requirements are the same as for regular contributions (see inside back cover).

Velocity of Bodies Powered by Diatomic Cold-Gas Thrusters

M.D. Bennett*
Sandia Laboratories, Albuquerque, N. Mex.

Nomenclature

b = mass-fraction parameter, $b=\lambda/(1-\lambda)$
c_i = initial sound speed in propellant gas (m/sec)
I_s = specific impulse of thruster (m/sec)
k = specific-heats parameter, $k=2/(\gamma-1)$
m_f = final vehicle mass (kg)
m_i = initial vehicle mass, including propellant gas (kg)
S = thruster nozzle throat area (m^2)
t = time (sec)
V = thruster reservoir volume (m^3)
$\mathcal{V}_S$ = vehicle normalized velocity, $\mathcal{V}_S=v/v_{t=\infty}$
v = vehicle translational velocity increment (m/sec)
β = specific-heats factor, $\beta=[(\gamma-1)/2][(\gamma+1)/2]^{-(\zeta/2)}$
γ = ratio of specific heats of propellant gas
ζ = specific-heats exponential factor, $\zeta=(\gamma+1)/(\gamma-1)$
θ = specific-heats factor, $\theta=[2/(\gamma+1)][2/(\gamma-1)]^{(1/2)}$
λ = vehicle mass fraction, $\lambda=m_f/m_i$
τ = normalized time, $\tau=1-[1/(1+\psi t)]$
ψ = thruster configuration parameter, $\psi=\beta S c_i/V$, (sec^{-1})

Introduction

In a previous investigation of the translational motion of a missile discharging an inert gas from a thermally insulated tank, an integral equation was derived that expressed the velocity imparted to the body when the working fluid expands isentropically through an infinite area ratio nozzle into a vacuum.[1] The analytical solution pertaining to the general case of arbitrary specific heats ratio had the form of an infinite series. For the particular and important category of fluids that yield integer values of the function $f(\gamma)=2/(\gamma-1)$, which corresponds to the molecular degrees of freedom in an ideal gas, a relatively simple algebraic expression was obtained. Finally, by way of example, the special solution was expanded to describe in detail the case involving the most elementary fluid in the category – the monatomic gases.

The expansion of the velocity equation for the next appropriate real fluid in the category – the diatomic gases – is summarized and compared with the previous results in the following discussion.

Integral Equation Expressing Velocity History

If the thermodynamic properties of the fluid inside the thruster reservoir maintain a uniform spatial distribution during the discharge process, the time-dependent gas dynamic equations may be analytically integrated to yield the pressure and temperature decay histories of a perfect gas with no thermal radiation, provided that the flow is assumed to be one dimensional, isentropic and quasi-steady. In accordance with that model, the equation describing the ideal velocity of the variable-mass system for the case of choked nozzle flow takes the form [see Eq. (7)]

$$v=\zeta I_s(\tau-\mathcal{I}_\tau) \tag{1}$$

where ζ denotes a factor involving the specific heats ratio, $I_s=\theta c_i$ represents the vacuum specific impulse of the thruster, and τ and $\mathcal{I}_\tau$ are the normalized time and a definite integral involving the normalized time, respectively.

The dimensionless integral $\mathcal{I}_\tau$ was previously found to be

$$\mathcal{I}_\tau=b^{(1/k)}\int_{\xi_1}^{\xi_2}\frac{d\xi}{1+\xi^k} \tag{2}$$

where $b=\lambda/(1-\lambda)$ is a known constant related to the propellant mass fraction, and $k=2/(\gamma-1)>1$. Equation (2) has the integration limits $\xi_1=(1/b)^{(1/k)}(1-\tau)$, $\xi_2=(1/b)^{(1/k)}$.

Solution of Velocity Equation

The solution for Eq. (2) involves an infinite geometric series when k is a noninteger. If, however, k may be specified as a positive integer, a simpler algebraic expression results. In the general form

$$\mathcal{I}_\tau=(b^{1/k}/k)\Big\{s\ln(\xi+1) -2\sum_{\mu=0}^{r-1}\Big[P_\mu\cos(\eta\pi/k)-Q_\mu\sin(\eta\pi/k)\Big]\Big\} \tag{3}$$

with $k=2r-s$, where $s=0$ or $s=1$. The trigonometric function's coefficients are

$$P_\mu=(1/2)\ln[\xi^2-2\xi\cos(\eta\pi/k)+1]$$

and

$$Q_\mu=\arctan[\xi\csc(\eta\pi/k)-\cot(\eta\pi/k)]$$

where $\eta=2\mu+1$.

According to the kinetic theory of gases for an elementary molecular model, the number of internal degrees of freedom, n, is given by the formula $n=2/(\gamma-1)$. Since the parameter $k=2/(\gamma-1)$ in Eq. (3) is identical to n, and, like n, is restricted to positive integers, certain values of $k=1,2,3,...,$ are equivalent to the number of degrees of freedom. Consequently, when only three degrees of freedom exist, $n=k=3$, and the normalized velocity of the constant entropy system takes the form

$$\mathcal{V}_S=\frac{\tau-A_\tau}{1-A} \tag{4}$$

where $A_\tau=(\mathcal{I}_\tau)_{k=3}$, and $A=(A_\tau)_{\tau=1}$. The expansion of the A_τ function in Eq. (4) is given in the cited reference, under the section "Monatomic Gases."

Received March 18, 1976; revision received April 7, 1976. This work was supported by the U.S. Energy Research and Development Administration.
Index categories: Missile Systems; Fuels and Propellants, Properties of.

*Member of the Technical Staff, Aerodynamics Department. Associate Fellow AIAA.

Table 1 Dimensionless velocity parameters for monatomic and diatomic cold-gas thrusters as a function of propellant mass fraction, $\lambda = m_f/m_i$

λ	$(1-A)$	$(1-B)$
0	1	1
10^{-7}	0.99439	0.95744
10^{-6}	0.98791	0.93255
10^{-5}	0.97395	0.89311
10^{-4}	0.94392	0.83060
10^{-3}	0.87954	0.73169
10^{-2}	0.74364	0.57610
0.1	0.47192	0.33767
0.2	0.35241	0.24638
0.3	0.27342	0.18870
0.4	0.21329	0.14591
0.5	0.16435	0.11169
0.6	0.12290	0.083080
0.7	0.086846	0.058454
0.8	0.054884	0.036806
0.9	0.026141	0.017475
0.99	0.0025108	0.0016743
0.999	0.00025011	0.00016674
0.9999	0.000025001	0.000016667
1	0	0

Diatomic Gases

In the case of a tank containing a compressed gas with five active degrees of freedom, the expression describing the ideal velocity becomes

$$\mathcal{V}_S = \frac{\tau - B_\tau}{1-B} \tag{5}$$

where $B_\tau = (\mathcal{J}_\tau)_{k=5}$ and $B = (B_\tau)_{\tau=1}$. From Eq. (3), the B_τ function is

$$(5/\eta)B_\tau = \ln(g_1 g_2 g_3) + 2\sin(\pi/5)\arctan(g_4) + 2\sin(3\pi/5)\arctan(g_5) \tag{5a}$$

where $\eta = b^{(1/5)}$, and the dimensionless g functions are

$$g_1 = (\eta+1)/(\eta+1-\tau)$$

$$g_2 = \{1 + [\tau^2 - 2(1-\eta\cos\pi/5)\tau]/[\eta^2 - 2\eta\cos(\pi/5) + 1]\}^{\cos(\pi/5)}$$

$$g_3 = \{1 + [\tau^2 - 2(1-\eta\cos 3\pi/5)\tau]/[\eta^2 - 2\eta\cos(3\pi/5) + 1]\}^{\cos(3\pi/5)}$$

$$g_4 = \eta\tau/\{\eta^2\sin(\pi/5) + [\eta\cot(\pi/5) - \csc(\pi/5)][\eta\cos(\pi/5) - 1 + \tau]\}$$

and

$$g_5 = \eta\tau/\{\eta^2\sin(3\pi/5) + [\eta\cot(3\pi/5) - \csc(3\pi/5)][\eta\cos(3\pi/5) - 1 + \tau]\} \tag{5b}$$

The arctan functions associated with the B_τ term in Eq. (5a) are restricted to the first and second quadrants.

The maximum velocity occurs at time $\tau = 1$, and amounts to $v_{t=\infty} = \zeta I_s(1-B)$. Written in terms of the initial speed of sound in the propellant gas, the terminal velocity is

$$v_{t=\infty} = 5^{3/2}(1-B)c_i \tag{6}$$

where $B = B(\lambda)$. The corresponding equation for missiles with thrusters using monatomic gases was previously shown to be $v_{t=\infty} = 3^{3/2}(1-A)c_i$.

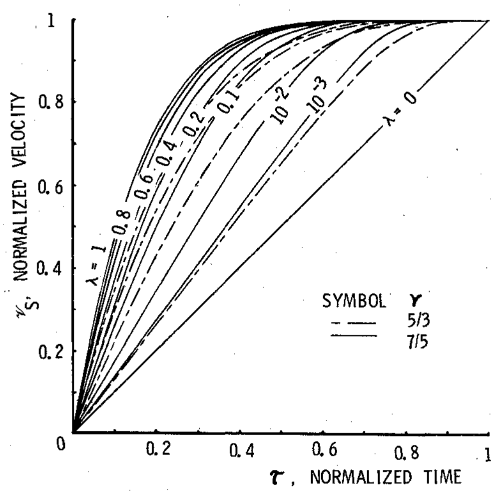

Fig. 1 Velocity history showing effect of propellant mass fraction λ. (The continuous-line curves represent diatomic gases, and broken lines represent monatomic gases. For clarity, only four cases are presented for the monatomic thrusters, which correspond to every other value of λ shown for diatomic systems; i.e., $\lambda = 0.01$, 0.2, 0.6 and 1.0. Curves describing the extreme condition of $\lambda = 0$ are straight lines of slope $\partial\mathcal{V}_S/\partial\tau = 1$, and are coincident for all working fluids.)

Results

The factor $(1-B)$ that appears in Eq. (6), together with the equivalent parameter for the monatomic gases, $(1-A)$, have been evaluated, and Table 1 summarizes the calculations. Applying these results, it is found that for relatively small quantities of the working fluid, a thruster employing the monatomic gas helium, for example, produces a velocity of approximately three-fourths that of a system using the diatomic gas nitrogen at the same initial pressure and temperature.

At the other extreme, where $\lambda = 0$, the resultant velocity remains finite. For the diatomic gases, this limiting velocity, i.e., the velocity attained by a body composed entirely of an inert propulsive fluid, is

$$v_{\lim} = 5^{3/2}c_i \tag{7}$$

By comparing Eq. (7) with the companion expression for monatomic thrusters ($v_{\lim} = 3^{3/2}c_i$), it is found that the maximum possible velocity obtainable from configurations containing the example gas nitrogen amounts to approximately three-fourths of that produced by helium systems at the same initial temperature.

The velocity determined from Eq. (5), together with the results for the monatomic gases, are shown parametrically in Fig. 1. It may be seen that for given values of $\lambda > 0$ and $0 < \tau < 1$, a decrease in γ has the effect of increasing the (normalized) velocity.

With this information, the time history of the ideal velocity may be readily calculated for thruster systems using monatomic or diatomic gases that are discharged at a sufficiently rapid rate to preclude significant heat transfer.

Range of Applicability

The departure in the behavior of a real gas from that of an ideal gas is dependent on the pressure, temperature, and type of gas. Most gases follow closely the ideal gas equation of state over the range of conditions of practical concern in thruster technology. Even as the working fluid expands to very low pressures, the gas is found to obey the ideal state equation because there is a simulataneous decrease in the density. Since the major portion of the impulse is delivered in the early time period, the degree of validity of the present results will be determined by the accuracy of the state equation, evaluated at the initial condition in the reservoir. For general purposes, satisfactory results are expected at temperatures up to 2,000K, which is considerably in excess of the temperature in current engineering designs.

Reference

[1] Bennett, M.D., "Velocity of Bodies Powered by Rapidly Discharged Cold-Gas Thrusters," *Journal of Spacecraft and Rockets*, Vol. 12, April 1975, pp. 254-256.

Stability of the Infrared Earth Horizon at 15μ

James William Hoffman*
Hughes Aircraft Company, El Segundo, Calif.

Introduction

FUTURE meteorological and Earth resources satellite missions involving high resolution imaging sensors will require extremely stable 3-axis attitude control systems. These systems, operating at synchronous altitude, will maintain a stable line of sight while a complete picture frame is imaged, in order to prevent picture distortion. Currently proposed systems will require an attitude reference measurement that is stable to within 1 to 2 arc sec over time periods up to 20 min long. The following experiment was performed to determine if the Earth horizon, in the 15μ region, could provide such a stable reference. If so, a simple Earth sensor could be used to provide long-term drift corrections for a gyro attitude reference system.

In this concept, the short-period attitude reference would be supplied by rate integrating gyros. The long-term attitude reference would be supplied by the horizon sensor through a very low bandwidth outer loop which smooths out the sample noise of the sensor.

Experiment Description

The method used to obtain the Earth horizon data was to utilize the video signals being telemetered to Earth from the Sun and Earth sensors aboard the Westar I Communications Satellite. Westar I is located in synchronous orbit at 99° west longitude. Although designed for another purpose, the Westar satellite provided a convenient means to conduct a preliminary investigation.

The north and south Earth sensors scan the Earth at 5° above and below the equator, with a 1.5° by 1.5° field of view, as the spacecraft spins at approximately 94 rpm. The Earth sensors are separated in spin angle (azimuth) by 45°. Each sensor employs a thermistor bolometer and a spectral filter with a 50% spectral bandpass of 13.9μ to 15.7μ. The signal is electronically filtered with a cut-on frequency of 0.5 Hz and a simple RC rolloff at 400 Hz. A typical detector has about 50 mv of noise. Both sensors are summed onto a single telemetry channel. With a 4 V signal the approximate signal to noise ratio (SNR) and single threshold position jitter (σ) caused by sensor noise alone are given by Eqs. (1) and (2).

$$\mathrm{SNR}_{\mathrm{typical}} \cong 4.0/(0.050\sqrt{2}) \cong 57 \tag{1}$$

$$\sigma \cong 1.3 \times 1.5 \text{ deg/SNR} \cong 0.034 \text{ deg} \tag{2}$$

Earth horizon stability is measured by recording the time between the center of an Earth pulse and the Sun pulse and multiplying by the current angular spin velocity of the spacecraft as shown in Fig. 1.

The current value of spin velocity is obtained by measuring the time between sun pulses. To this value, correction terms are then added to account for 1) the apparent movement of the sun throughout the day θ_s; 2) the effect of orbit eccentricity on orbital rate; 3) the movement caused by Earth triaxiality acceleration θ_T; and 4) Earth parallax θ_p. Spacecraft nutation and attitude error all vary the length of the earth chord. The effect of this variation is eliminated by measuring to the center of each chord. The equations used are:

$$\epsilon_n = (T_1 + T_2)(\pi/T_s) + \theta_s + \theta_T + \theta_p \tag{3}$$

$$\theta_s = -4\pi \sum_{y=1}^{n} \left[T_{s(y)} / [T_{0(y)} - T_{s(y)}] \right] \tag{4}$$

$$T_{0(y)} = 86{,}400/[1 + 0.00044531 \cos [2\pi(t + t_0)/86{,}400]] \tag{5}$$

$$\theta_T = 2.68 \times 10^{-16} t^2 \tag{6}$$

$$\theta_p = 2.818 \times 10^{-4} \sin(\pi t_m / 43{,}200) \tag{7}$$

where T_s is instantaneous spin period of spacecraft (sec), T_0 is instantaneous orbital period of Earth (sec), t is time from start of experiment (sec), t_0 is time from orbit perigee to start of experiment (sec), and t_m is time from midnight (satellite time) (sec).

In order to make the timing circuits insensitive to long-term gain changes in the sensor, adaptive thresholding circuits were employed. These circuits set the thresholds at 50% of the pulse amplitude as measured on a previous pulse.

Results

Figures 2a and 2b show the results obtained over four separate days for the north limb and south limb, respectively. Valid data was not obtained around midnight because of the overlapping in time of the Sun and Earth pulses, which are transmitted to Earth on the same telemetry line. This interference problem (plus ground station uncertainties) could be eliminated by a dedicated experiment that employed on-board thresholding. It can be seen that at the beginning of most daily runs, a large transient occurred in the data after coming out of this interference period. These transients are most likely caused by electronic or processing effects in the experimental setup.

Before plotting, the data was smoothed by 1000 points or approximately 20 min of data (measurements were made on alternate spin cycles). A least squares regression was then performed on the data using both a 12 hour sinusoid and a 24 hour sinusoid. The 12 hour sinusoid provided the better fit and is shown (with rectangles) superimposed on the actual data. The average amplitude of the 12 hour sine wave fit for all 4 days and both sensors was 74.5 μr. The maximum change in angle for this average sinusoid over any 20 minute period is 13.0 μr as shown below in Eq. 8.

$$\Delta\theta_{\max} = 74.5\mu\mathrm{r}(2\pi/720)20 = 13.0\mu\mathrm{r} \tag{8}$$

If it is postulated that there are no significant high frequency fluctuations in the 935 km square portion of the atmosphere seen by the sensor, then this 13 μr fluctuation would represent the maximum 20 minute drift in the attitude reference.

Single threshold position jitter was computed for the data run of 23 May as a check on initial sensor accuracy estimates.

Received March 19, 1976; revision received May 3, 1976. The author wishes to acknowledge the assistance of F. Hummel, R. Eiermann, M. Hall, M. Lyon, E. Sachtleben, and B. Thomas in carrying out the experiment.

Index categories: Atmospheric, Space and Oceanographic Sciences; Earth Satellite Systems, Unmanned; Spacecraft Attitude Dynamics and Control.

*Senior Systems Engineer, Systems Laboratories, Space & Communications Group.